AD-A051 988 UNIVERSITY OF SOUTHERN CALIFORNIA LOS ANGELES DEPT O--ETC F/G 20/12
THE STRUCTURAL CHARACTERISTICS OF RADIATION DAMAGE PRODUCED BY --ETC(U)
1977 G H NARAYANAN, W C SPITZER F44620-76-C-0061

UNCLASSIFIED AFOSR-TR-78-0407 NL

| OF |
AD
A051988

END
DATE
FILMED
5-78
DDC

THE STRUCTURAL CHARACTERISITICS OF RADIATION DAMAGE PRODUCED BY HIGH ENERGY (2.7 MeV) ION IMPLANTATION IN GaAs

G. H. Narayanan and W. G. Spitzer
Department of Materials Science
University of Southern California
Los Angeles, California 90007

ABSTRACT

The radiation damage induced by the implantation of 2.7 MeV P^+ and N^+ ions with a dose of 6.4×10^{16} ions/cm^3 into GaAs at room temperature has been studied by transmission electron microscopy. The as-implanted material was found to consist of a buried amorphous layer which was sandwiched between a heavily damaged but crystalline cover layer exhibiting a high density of black dot defects, microtwins and dislocation loops and a less damaged substrate region. Post-implantation annealing of the specimens at 250°C for 6 hours resulted in the recrystallization of the amorphous and cover layers by random nucleation of grains producing a polycrystalline region on the single crystal substrate. However, a second stage annealing of these samples at 400°C for 2 hours caused an epitaxial regrowth of the implanted layer on the undamaged substrate producing single crystal regions which were heavily twinned on all {111} planes. The results of the present microstructural analyses have been compared with the previous infrared reflectivity studies on identically implanted GaAs samples to determine the effects of structural changes on the dielectric properties. The two studies are found to be in reasonable agreement.

1. INTRODUCTION

Ion implantation of dopant atoms has now been successfully employed to produce both p-type and n-type layers on GaAs substrates. High energy implantation, however, introduces considerable damage to the host lattice, the extent of which is determined by the mass, energy and dose of the implanted ions the mass of the target atoms as well as the temperature of the target. In extreme cases, the atomic disorder in the implanted region can be sufficiently great as to cause crystalline-to-amorphous transitions to occur. Any impurity conduction effect arising from the electrical (doping) characteristics of the implanted ion is generally completely masked by the damage. Therefore the damage must be annealed out by appropriate post-implantation heat treatment which will reduce the residual defects to a level where carrier mobilities and lifetimes are usefully large and the implanted ions will be incorporated into electrically active sites in the crystal lattice. Thus, it is of great interest to study the nature of implantation induced damage as a function of implantation conditions and the recovery of the damage during post implantation annealing.

In some recent studies of ion-implanted GaAs by Kachare et al. (1,2,3) demonstrated that the implantation induced changes in optical properties can be used as a tool to characterize the extent of the damage produced by the implantation. More specifically, it has been shown that the near-infrared refractive index of GaAs can be substantially increased by the lattice damage caused by large dose ion-implantation and that these changes in refractive indices exhibit a depth distribution related to that of the damage concentration (2,3). The room temperature near-infrared reflection and transmission were measured over a wide range of photon energies on GaAs implanted at 2.7 MeV P^+ ions with a fluence of $6.4 \times 10^{16}/cm^2$, and these measurements revealed

interference fringe patterns which were strongly amplitude modulated. It has been shown by Kachare et al. (2,3) that the reflection fringes could be analysed in terms of a simple model in which the implanted material was approximated by a heavily damaged and buried layer sandwiched between a partially absorbing cover layer and a non-absorbing substrate. A detailed analysis of the measured fringe patterns by using a curve fitting procedure indicated that the effective layer thicknesses were comparable to those predicted by the projected range of the ions and width of the gaussian ion distribution. Annealing of the specimens at $\lesssim$ 400°C resulted in a reduction in implantation-induced changes in refractive index, with the buried and cover layers becoming optically essentially the same, indicating the removal of the damage during annealing. The implant layer thickness, on the other hand, remained unchanged. The general conclusions of this study was that the implantation induced damage in GaAs does not primarily anneal out by an epitaxial regrowth process as has been observed for heavily implanted Si, at least in the temperature range investigated.

Although optical measurements of the type described above give some idea about the extent of the damage no precise information regarding the structural characteristics of the damage can be deduced. In the present investigation, therefore, transmission electron microscopy was used to study the lattice damage induced by the implantation of 2.7 MeV P^+ and N^+ ions in the GaAs samples. These samples are the same or identical to those which were previously studied by the optical properties measurement techniques. The microstructural changes accompanying the post-implantation annealing treatments at 400°C and below have been followed to establish the processes involved in the elimination of the implantation induced damage.

The results indicate that the ion implanted region in these GaAs samples consists of an amorphous layer buried below a heavily damaged crystalline cover layer, thus confirming the layer model proposed by Kachare et al. (2,3). The removal of the damage during post-implantation annealing at 250°C is shown to occur by the recrystallization of both the buried amorphous and crystalline cover layers which results in the formation of a polycrystalline surface layer. A different annealing mechanism is shown to operate during a second stage annealing at a higher temperature viz. 400°C, by which a regrowth of the damaged layer occurs epitaxially on the substrate as has been observed for heavily implanted Si having the same orientation (4).

2. EXPERIMENTAL PROCEDURE

The details of the procedure for ion implantation of GaAs used in this study are essentially those described in previous papers (2) and therefore only a brief description will be included here. Wafers of GaAs cut from undoped ingots were initially mechanically polished to 0.5mm thickness. One surface of the wafer was then chemically polished to remove the surface damage. The polished surface was implanted with $^{31}P^+$ $^{14}N^+$ ions by using the Van de Graaff accelerator at the Rome Air Developmental Center, Hanscom Air Force Base. During implantation the wafers were mounted on a water cooled holder with a thin layer of vacuum grease between the lapped specimen surface and the holder to improve the thermal contact. One wafer, having <100> orientation was implanted with $^{31}P^+$ ions having an energy of 2.7 MeV at a dose rate of 1.3×10^{12} ions/cm^2 sec to give a total dose of 6.4×10^{16} ions/cm^2. A second wafer having a <110> orientation was implanted with 3.0 MeV $^{14}N^+$ ions and a total dose of 2.0×10^{17} ions/cm^2. After the implantation the samples were cleaned with a 50-50 toluene-methanol

mixture and any residual carbon deposit removed by 15 to 30 min. of cold oxygen plasma treatment. Post-implantation annealing of the samples was carried out in cleaned, evacuated sealed quartz ampoules, at 250°C and 400°C.

From the as-implanted and the annealed GaAs, specimens 3x3 mm^2 in size, suitable for transmission electron microscopy were cut with a wire saw. It has been shown from previous studies (2,3) that the region of maximum lattice damage in 2.7 MeV P-implanted samples occurs as a buried layer of $\sim$ 0.3 μm in thickness beneath a cover layer of $\sim$ 2 to 2.3 μm in thickness. Therefore a two stage thinning procedure involving both ion beam milling and chemical jet polishing steps was used to insure that the buried layer was included in the thin foil specimen. Ion beam milling was initially employed to remove in a controlled manner a layer $\sim$ 2μ in thickness from the implanted side. Final thinning to electron transparency was accomplished by chemical jet polishing from the substrate side. All specimens were examined in a Hitachi HU-125 transmission electron microscope operated at 125 KV with the implanted side facing the incident electron beam.

3. RESULTS

3.1 As-Implanted Material

Figure 1(a) shows a typical electron diffraction pattern obtained from the heavily damaged region of a GaAs specimen implanted with $^{31}P^{+}$ ions having an incident energy of 2.7 MeV and a total dose of 6.4×10^{16} ions/cm^2. This heavily damaged region, occurs at a depth of 2μ below the original surface which roughly corresponds to the position of the peak in the depth distribution of the implanted species in the specimen. The pattern in Fig. 1(a) is composed of three diffused rings

or halos surrounding the central spot, and is characterisitic of those produced by amorphous films. Thus it is quite evident that implantation of high energy P^+ ions in large doses has driven GaAs in this region into an amorphous state.

The electron transparent region of the specimen had a wedge-shaped profile as illustrated in Figure 1(b). The diffraction pattern shown in Figure 1(a) was obtained from the thinnest regions of the foil, which consisted only of the amorphous layer. The patterns taken from the adjacent thicker areas of the foil revealed, in addition, the presence of diffraction spots arising from crystalline GaAs which were superimposed on the diffused rings from the amorphous layer. An example is shown in Figure 1(c). It can be noticed that the strong diffraction spots are also circled by diffused rings. This is clearly a double diffraction effect whereby the strong diffracted beams originating from the crystalline region act as new sources for further diffraction from the amorphous region. Since in the present study all the specimens were examined in the microscope with the implanted side facing the incident electron beam, the above observation clearly implies that overlaying the amorphous region there exists a relatively less damaged crystalline layer.

The spot pattern shown in Figure 1(c) can be indexed as that due to GaAs, which is tilted off the exact <100> orientation about a <022> axis. An additional feature of this pattern is the presence of four satellite spots around each of the matrix reflections that lie on either side of the tilt axis. These satellite spots which are elliptical in shape are displaced from the matrix reflection along the <022> directions. Tilting the specimen to exact <100> orientation caused these satellite

spots to disappear, indicating that they do not lie in the {100} reciprocal lattice plane. Pashley and Stowell (5) have shown that the reciprocal lattice points due to twins occuring on all the {111} planes of an fcc matrix either coincide with the matrix spots or are displaced from the matrix spots by vectors of ± 1/3 <111>. As a consequence of the equivalence of the fcc and sphalerite lattices, the above analysis is also applicable to the present case. In addition, if the twins are in the form of thin platelets (which is the case with microtwins), the twin reciprocal spots will be streaked along the <111> directions. These <111> streaks will intersect the {100} matrix reciprocal lattice plane obliquely. The origin of the elliptical satellite spots which are displaced along the <011> directions in the <100> diffraction pattern can now be understood in terms of the intersection of these <111> streaks with the sphere of reflection as illustrated schematically in Fig. 1(d).

The existence of the microtwins was confirmed further by darkfield imaging. Fig. 2 shows a typical darkfield micrograph obtained by imaging a prominant satellite reflection (indicated by the arrow in Fig. 1 (c)), revealing the microtwins. This micrograph also reveals the boundary region between the completely amorphous area and the adjoining regions with the crystalline cover layer. As can be noticed, the microtwins are confined primarily to the region close to the amorphous crystalline interface.

A closer examination of the crystalline cover layer, which is approximately 2 μm thick, by preparing additional thin foil specimens showed that this region is characterized by a high density of "black dot defects." These are characteristic of radiation damage induced in crystalline material by high energy particles (6). A typical example of this is shown in Fig. 3(a), which is a brightfield micrograph obtained from the cover layer, removed from the amorphous crystalline interface. The crystalline nature of the cover layer is evident from the selected area electron diffraction pattern.

The density of the "black dot defects" decreased somewhat with increase in distance from the interface. Fig. 3(b) shows a typical bright-field micrograph obtained from a region close to the implanted surface. The "Black dot defects" in this region exhibit black/white contrast (Fig. 3(b)) which is typical of the image contrast produced by point defect clusters under two beam dynamical condition. In addition to the "black dots defects", small prismatic dislocation loops with characteristic line of no-contrast perpendicular to the diffraction vector can also be noticed in this region (indicated by the arrows in Fig. 3(b). Although the exact nature of these defects have not been unambiguously determined, they are believed to be caused by the condensation interstitial clusters.

The type of crystal defects observed in the region immediately below the amorphous layer (viz., in the crystalline substrate regions) were in general similar to those observed in the cover layer. However, this region was also characterized by the presence of thin platelike or disc shaped precipitates, which exhibited rather poor contrast as can be seen in Fig. 3(c). These precipitates are more clearly resolved in darkfield images formed by weak beam techniques (Fig. 3(d)). Since these precipitates did not produce any detectable effect in the selected area diffraction patterns, a positive identification of their exact nature could not be made.

Finally, under the conditions of high incident energies and heavy doses employed in the present studies, the specific ion used for implantation appears to play a relatively minor role in determining the nature and extent of the implantation induced damage in GaAs. The general conclusions regarding the lattice damage produced by the implantation of $^{31}P^{+}$ ions, have been found to be valid also in the case of GaAs specimens implanted with $^{14}N^{+}$ ions.

III(b) Effects of Post Implantation Annealing

The recovery of the 2.7MeV P^+ ion implantation induced lattice damage during post implantation annealing treatments has been also followed by using electron microscopy. The heat treatment schedules employed here are exactly identical to those used in the previous infrared reflectivity studies (2, 3) on identically implanted material. One set of samples was annealed at 250°C for 6 hours while a second set was given an additional treatment at 400°C for 2 hours.

Figure 4(a) shows a typical electron diffraction pattern obtained from the implanted layer following annealing at 250°C for 6 hours. As can be noticed, the pattern is composed of spotty rings, characteristic of a moderately fine grained polycrystalline structure. A closer examination of this diffraction pattern shows that rings corresponding to the reflections from the {200} {222} and {420}planes of the GaAs lattice are clearly absent and that distinct maxima occur on several of the rings that are present. The latter observations can be taken as an indication of the existence of some degree of preferred orientation of the recrystallized grains. Furthermore, it can be noticed that the spots on the rings in many cases are streaked along a particular direction and that a similar streak also appears at the origin (i.e. central spot). These streaks must be associated with the shape of individual crystallites, which can be best described as 'thin platelike' from the brightfield images (Fig. 4(b). The exact size and shape of the individual crystallites can be better revealed by forming darkfield images of the intense difraction spots appearing on the rings. Figure 4(c) is a typical darkfield micrograph obtained from, this specimen which shows the presence of thin platelike crystallites having an irregular shape. Details of the defect structure within the individual crystallites could be clearly resolved owing to the presence of a high density of residual defects in them.

The annealing at 250°C for 6 hours was found to cause the recrystallization of both the buried amorphous and crystalline layers. The recrystallized polycrystalline layer, thus, extended from the original amorphous layer substrate interface clearly to the surface, thereby eliminating the prior distinction between the cover and burried layers.

The crystallography and morphology of the implanted layer in samples which have been subjected to a second stage annealing at 400°C for 2 hours were found to be distinctly different from those described above. The electron diffraction patterns obtained from these samples (Fig. 5(a)) revealed that the recrystallized layer was essentially single crystal. The pattern shown in Fig. 5(a) can be indexed as that due to a <100> oriented GaAs single crystal indicating that the regrowth of the damaged layer occurred epitaxially with the undamaged crystalline substrate. The brightfield micrographs of the regrown layer (Fig. 5(b)) showed that the morphology was drastically different from that observed after the first stage anneal and that the substructure was quite complex. In order to identify the nature of the substructure, further diffraction analysis was carried out. Tilting the specimen off the exact <100> orientation about a (002) axis was found to bring up additional satellite spots which were not in the (100) reciprocal lattice plane. This is illustrated in Fig. 6(a) which shows extra spots displaced from the original matrix reflections along the two perpendicular <022> directions. As was discussed in section 3.1, the elongated elliptical shape of these satellite spots indicates that they arise from the intersections of the sphere of reflections with <111> streaks, and that these streaks probably arise from microtwins in the {111} orientations. This interpretation is further supported by the results of the darkfield analysis. Fig. 6(b) and (c) are two darkfield micrographs obtained by imaging the satellite reflections

1 and 2 [indicated by the arrows in Figure 6(a)] respectively, which reveal the microtwins in two different {111} orientations.

In addition to the microtwins, other residual defects such as small prismatic dislocation loops and precipitates could be also observed in the microstructure. Figure 6(d) is a high magnification brightfield micrograph revealing this feature. Owing to the complexity of the substructure a detailed analysis of the nature of these loops and precipitates was not carried out.

IV. Discussion

It is interest to compare the results of the present microstructural measurements with those of the previous infrared studies in an attempt to determine the effect of the structural changes on the dielectric properties. In general, the two studies are in reasonable agreement although the present results will modify one of the principle conclusions of the infrared investigation. First let us consider the as-implanted material. The present electron microscopy studies have shown that the three-layer model for the implanted material proposed earlier by Kachare et al. is essentially correct. Implantation of 2.7 MeV $^{31}P^{+}$ ions at high doses, is shown to produce an amorphous layer, which is buried ~2μm below the original surface of the sample. Since the diffraction pattern obtained from this layer (Figure 1(a)) shows a reasonably well-defined ring structure, it can be inferred that the structure must still possess some degree of short range order. This is because for a truly amorphous structure, it should be virtually impossible to distinguish these rings from each other. The radii of the various rings observed in the diffraction pattern were measured accurately by carrying out optical densitometer traces across the diffraction pattern and the "d" spacing corresponding to each ring was calculated by using the camera contrast. The estimated values of interatomic spacings for the different rings are shown in Table I. The Bragg

spacings corresponding to the three Debye rings show appreciable deviations from the "d" spacing for the crystalline material. Deviations of a similar nature have been reported also in the case of amorphous Si produced by ion implantation where it was shown that the amorphous material was ~7% less dense than crystalline Si [7].

While no precise measurement of the extent of the buried layer was made, its position was found to correspond roughly with that deduced from the previous infrared reflectivity measurements. The cover layer, which extends from the amorphous layer to the surface of the specimen was found to remain essentially crystalline, although this region was heavily damaged as characterized by the presence of a high density of "black dot defects." The crystalline substrate regions immediately below the amorphous buried layer, on the other hand, was shown to contain an unidentified precipitate phase.

The infrared measurements of essentially identical non-annealed samples gave refractive indices for the cover and buried layers of 3.58 and 3.66, both substantially larger than the 3.30 value for the non-implanted GaAs. Assuming the crystalline cover-to-amorphous buried layer interface is thin compared to be infrared wavelength in the material, then the refractive index of heavily damaged but crystalline material can be much closer to that of amorphous material than to the undamaged, crystalline value.

An interesting result that emerged from this investigation is the demonstration that the observed recovery and recrystallization of the damaged layer (viz. cover and buried layers) proceeds during post-implantation annealing by different processes at 250°C and 400°C. The first stage annealing at 250°C for 6 hours was shown to result in the recrystallization of the amorphous and cover layers by random nucleation of feathery or thin platelike grains producing a poly-

crystalline layer on the undamaged substrate. This process also eliminated the distinction between the cover and buried layers, and is similar to that envisaged by Kachare et al. (3) based on their infrared reflectivity and x-ray diffraction analyses. The refractive indices of the cover and buried layers moved close to the non-implanted value of 3.30 after the recrystallization. This indicates that the damage level in the recrystallized polycrystalline material is much less than that in the as-implanted crystalline cover layer, at least in the region of high "black dot defect" density which should be influencial in determining the apparent refractive index change at the crystalline-amorphous interface. Thus here also the two studies are in substantial agreement.

A major conclusion of the infrared study was that there was no evidence for epitaxial recrystallization. However after subsequent annealing at 400°C the interference fringes were gone in one case and much reduced in another, and it was assumed that this was the result of further annealing of damage which remained after the 250°C anneal. It is now observed however, that an epitaxial recrystallization of the polycrystalline material takes place at 400°C through a regrowth of the implanted layer on the undamaged substrate. This latter recrystallization process is similar to that reported for high temperature annealing of heavily implanted silicon.[4] While the regrowth leads essentially to the formation of a single crystal, the regrown layer was found to contain a high density of microtwins and other types of lattice defects. Differences in the quality of the regrown materials could lead to differences in refractive indicies and thus might explain the different results observed in the infrared studies.

V. ACKNOWLEDGEMENTS

The research in part was sponsored by the Joint Services Electronics Program through Air Force Office of Scientific Research (AFSC) under contract F 44620-76-C-0061.

REFERENCES

1. A. H. Kachare, W. G. Spitzer, F. K. Euler and A. Kahan, J. Appl. Phys. 45, 2938 (1974).

2. A. H. Kachare, W. G. Spitzer, J. E. Fredrickson, J. Appl. Phys. 47, 4209 (1976).

3. A. H. Kachare, W. G. Spitzer, J. F. Fredrickson and F. K. Euler, J. Apply Phys. 47, 5374 (1976).

4. L. Csepregi, J. W. Mayer, T. W Sigmon, Phys. Lett. A 54, 157 (1975).

5. D. W. Pashley and M. J. Stowell, Phil. Mag. 8, 1605 (1963).

6. M. Ruhle, M. Wilkens and V. Essmann, Phy. Stat. Sol. 11, 819 (1965).

7. D. J. Mazey, R. S. Nelson and R. S. Barnes, Phil. Mag. 17, 1145 (1968).

A COMPARISON OF THE ESTIMATED "d" SPACINGS CORRESPONDING TO THE DIFFUSED RINGS IN THE DIFFRACTION PATTERN FROM AMORPHOUS GaAs WITH THOSE FOR CRYSTALLINE GaAs

TABLE I

	d spacings (A°)		
	Ring 1	Ring 2	Ring 3
Present Work	3.30	1.91	1.25
Crystalline GaAs	3.264 (111)	1.999 (220)	1.154 (224)

FIGURE CAPTIONS

Figure 1 (a) A Transmission Electron Diffraction obtained from the heavily damaged region ~ 2μ below the surface of a 2.7 MeV P^+ implanted GaAs specimen.

(b) A schematic diagram of the cross section of a tapered thin foil specimen showning the layered structure produced by 2.7 MeV P^+ implantation.

(c) An electron diffraction pattern obtained from the thicker region of the foil (marked by the dotted circle in Figure 1(b)) showing the presence of a heavily twinned crystalline cover layer above the amorphous layer.

(d) A schematic diagram illustrating the origin of the elliptical satellite reflections in Figure 1(c) in terms of the intersection of {100} reciprocal lattice plane with the sphere of reflection.

Figure 2 A dark field micrograph obtained by imaging a twin reflection (indicated by the arrow in Figure 1(c)) showing the presence of microtwins.

Figure 3 (a) Brightfield Electron micrograph obtained from the crystalline cover layer region in the 2.7 MeV P^+ implanted GaAs specimen showing the distribution of lattice damage. The selected area electron diffraction pattern from this region is shown as an insert.

(b) Brightfield micrograph obtained from a region closer to the surface than the one in Figure 3(a). Arrows indicate small prismatic dislocation loops.

(c) Brightfield micrograph showing the presence of unidentified precipitates in the substrate regions below the amorphous layer

(d) Dark-field micrograph corresponding to the area in Figure 3(c).

Figure 4 (a) Electron diffraction pattern from the implanted layer in a P^+ implanted specimen following annealing at 250°C for 6 hours showing its fine-grained polycrystalline nature.

(b) Brightfield micrograph corresponding to Figure 4(a) showing the morphology of the recrystallized polycrystalline layer.

(c) A Dark-field micrograph obtained by imaging a segment of the bright diffraction ring in Figure 4(a) showing shape of the individual crystallites.

FIGURE CAPTIONS

Figure 5 (a) Electron diffraction pattern from the P^+ implanted layer following the two stage annealing (viz. 250°C-6 hours + 400°C 2 hours) showing its single crystalline nature of the regrown layer and its epitaxy with the <100> substrate

(b) Bright-field micrograph showing the morphological features of the regrown layer.

Figure 6 (a) Diffraction pattern obtained by tilting the specimen off the exact <100> orientation about the [002] axis showing the evolution of satellite reflections around the matrix reflections due to twinning on all {111} planes.

(b & c) A dark-field micrograph obtained by imaging the twin refelctions 1 and 2 respectively of Figure 6(a) showing two different variants of the twin lamalle.

(d) A high magnification bright-field micrograph showing the residual defects in the regrown layer.

FIG. 1

a

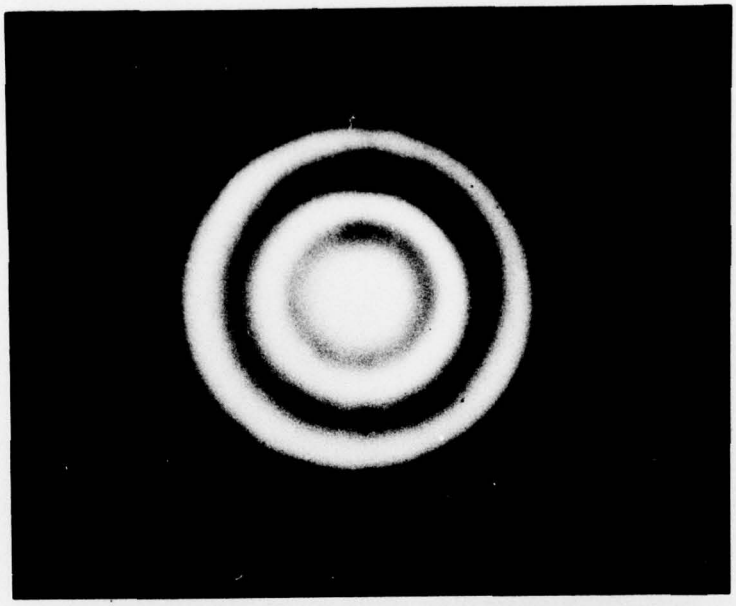

b

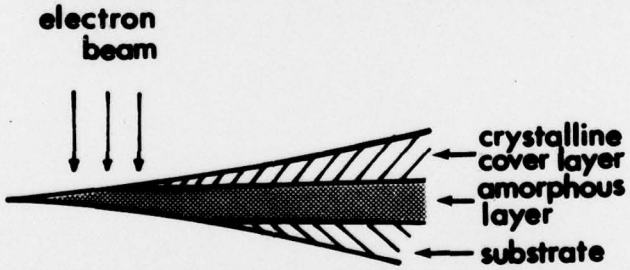
electron
beam
crystalline
cover layer
amorphous
layer
substrate

c

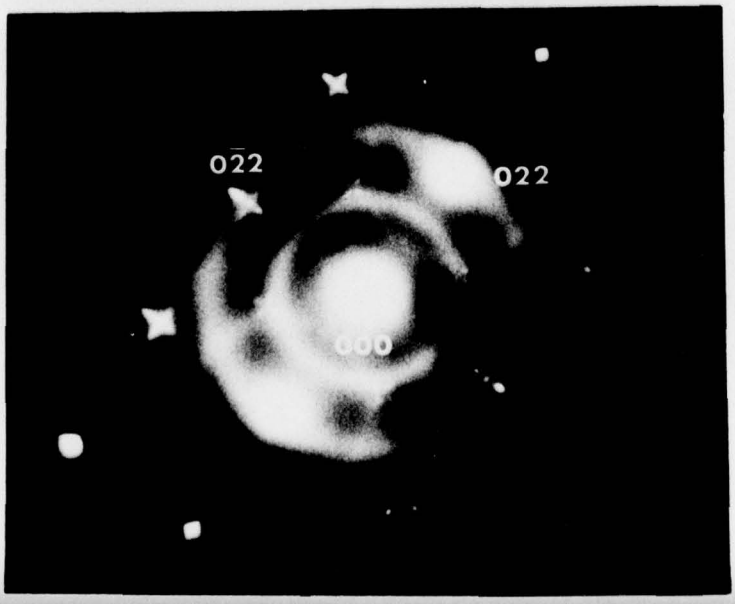
0$\bar{2}$2
022
000

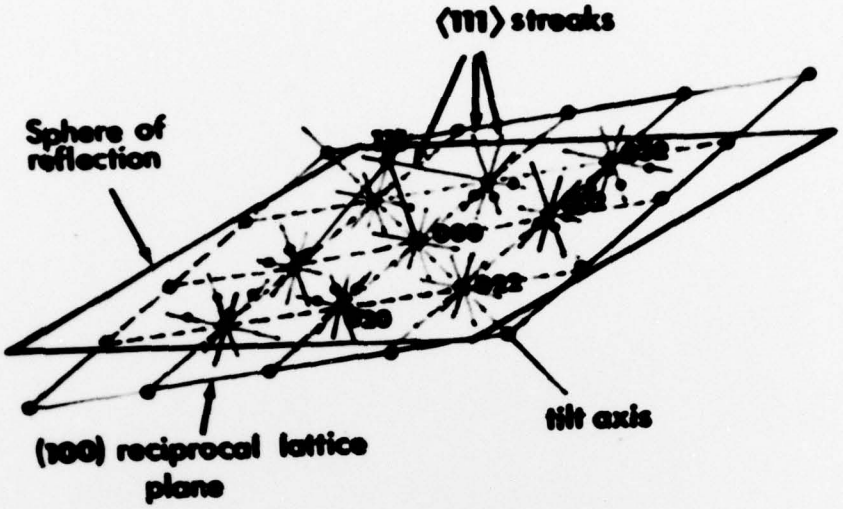
⟨111⟩ streaks
Sphere of reflection
tilt axis
(100) reciprocal lattice plane

1 (d)

FIG. 2

FIG. 3

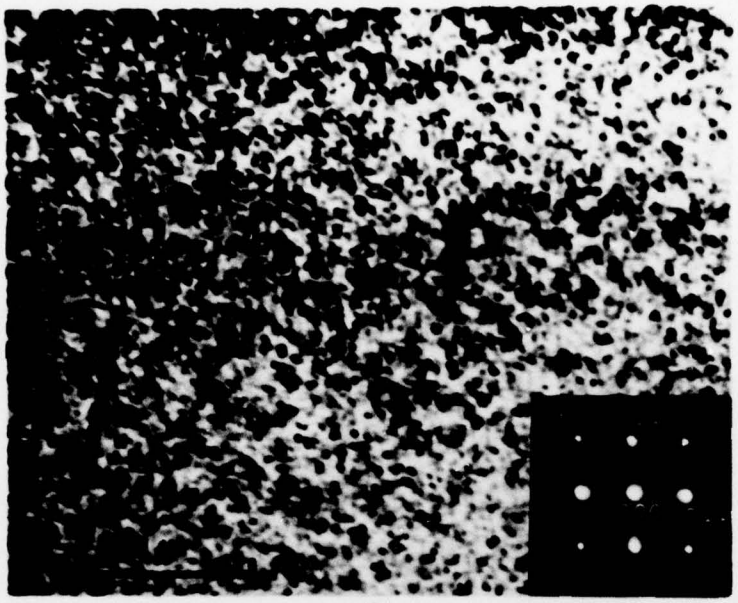

a

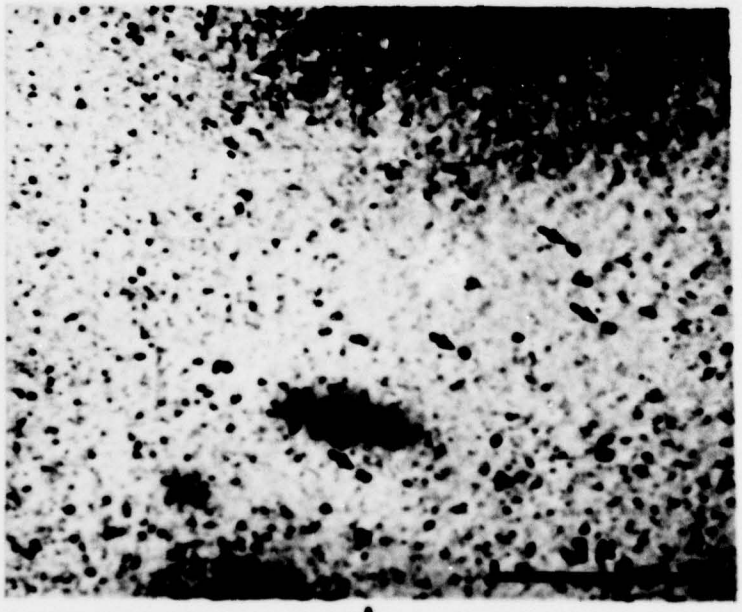

b

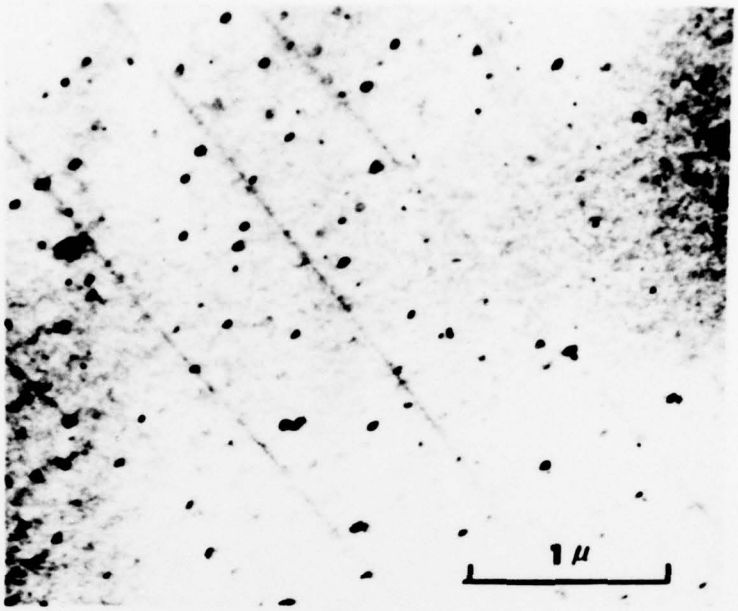

3c

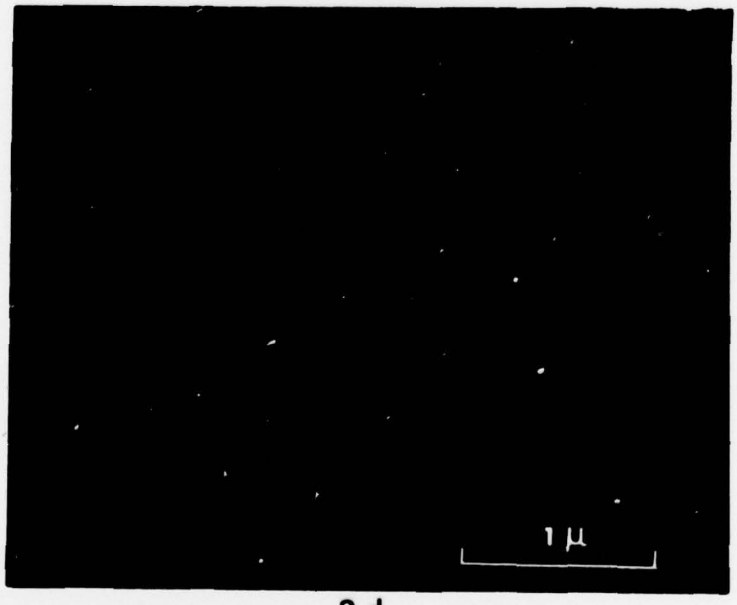

3d

FIG. 4

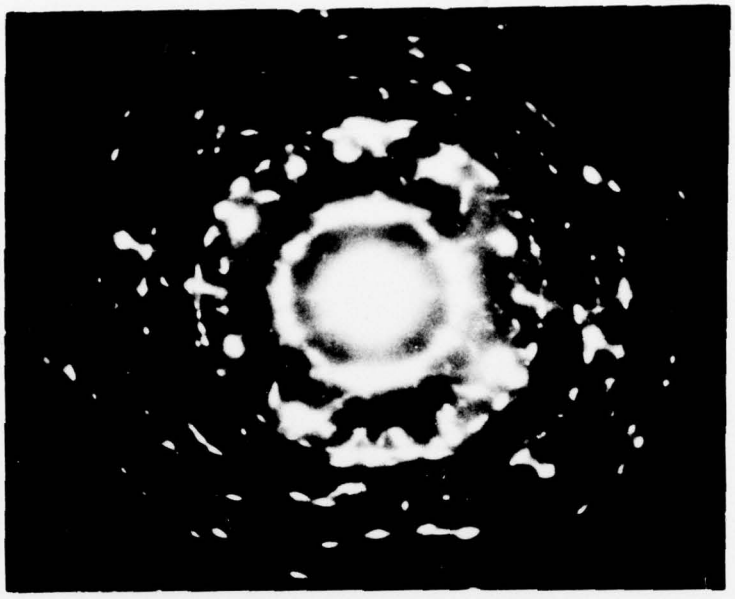

a

b

c

FIG. 5

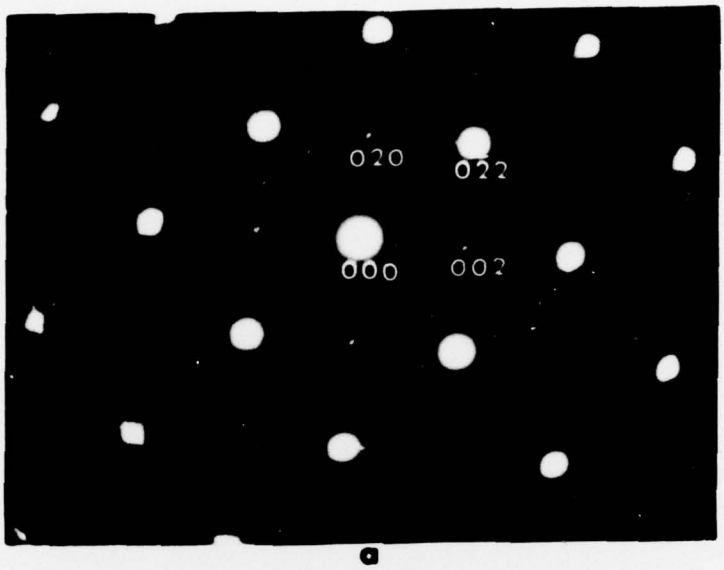

a

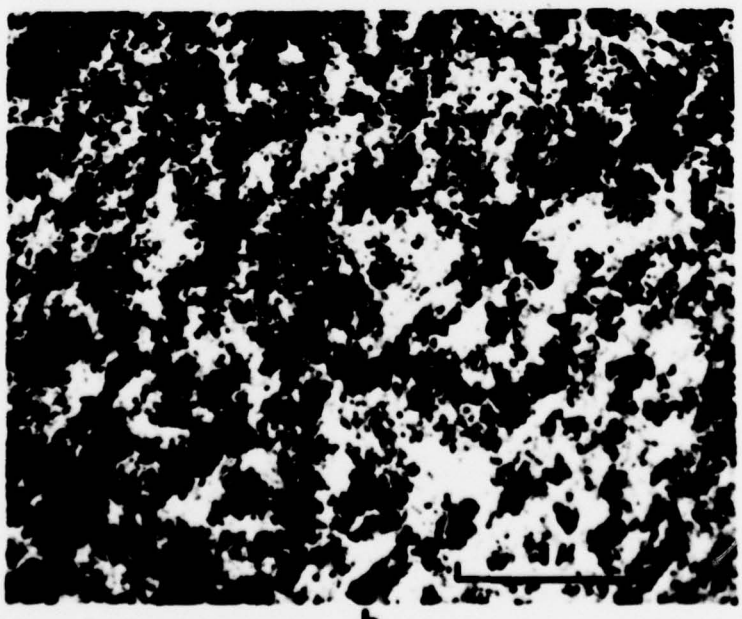

b

FIG. 6

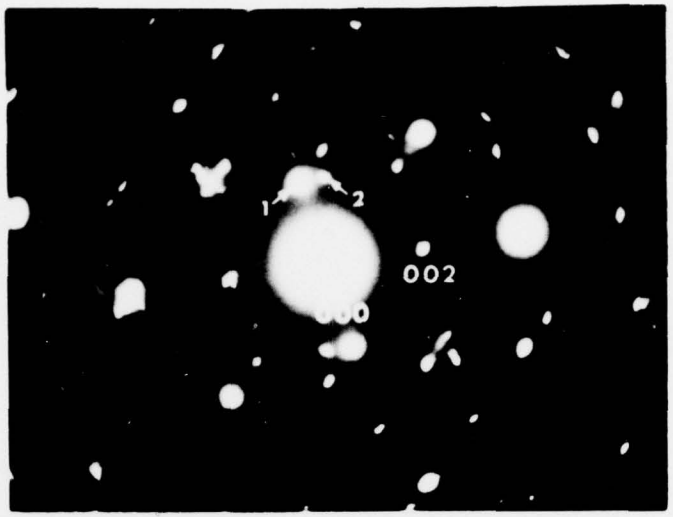

a

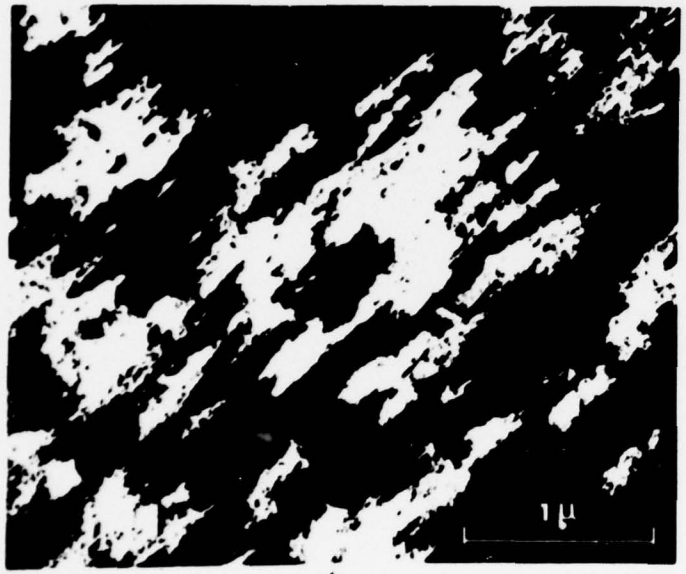

b

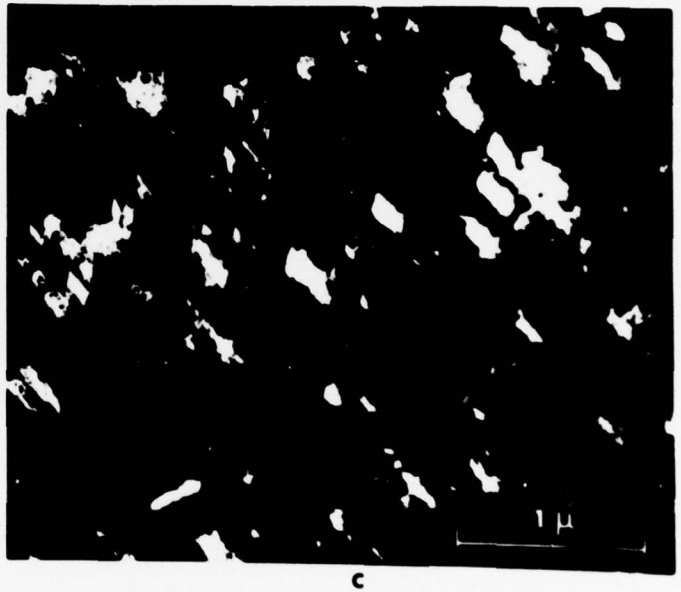

c

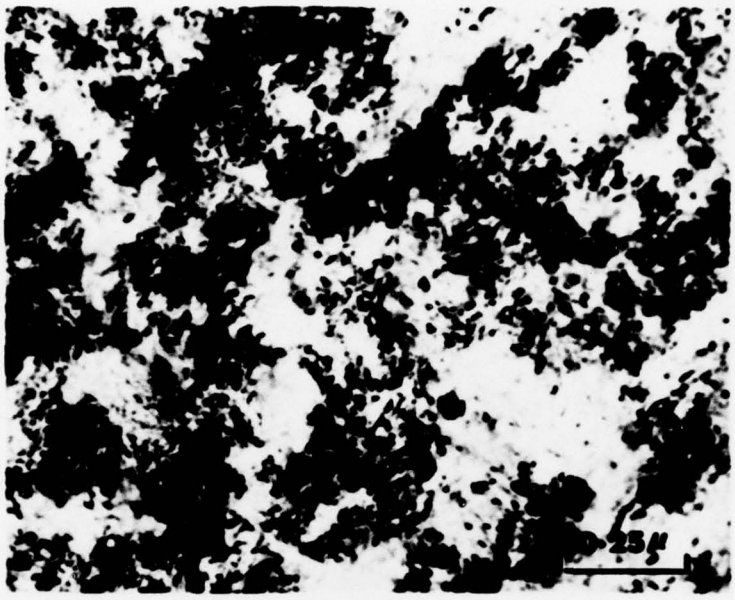

6 d

SECURITY CLASSIFICATION OF THIS PAGE (When Data Entered)

REPORT DOCUMENTATION PAGE

READ INSTRUCTIONS BEFORE COMPLETING FORM

1. REPORT NUMBER: AFOSR-TR-78-0407
2. GOVT ACCESSION NO.
3. RECIPIENT'S CATALOG NUMBER

4. TITLE (and Subtitle): The Structural Characteristics of Radiation Damage Produced by High Energy (2.7 MeV) ION Implantation in GaAs
5. TYPE OF REPORT & PERIOD COVERED: INTERIM rept.
6. PERFORMING ORG. REPORT NUMBER

7. AUTHOR(s): G. H. Narayanan and W. C. Spitzer
8. CONTRACT OR GRANT NUMBER(s): F44620-76-C-0061

9. PERFORMING ORGANIZATION NAME AND ADDRESS: Department of Materials Science, University of Southern California, Loa Angeles, California 90007
10. PROGRAM ELEMENT, PROJECT, TASK AREA & WORK UNIT NUMBERS: 2305/A9, 61102F

11. CONTROLLING OFFICE NAME AND ADDRESS: Air Force Office of Scientific Reaserch, Bldg. 410 Bolling AFB DC 20332
12. REPORT DATE: 1977
13. NUMBER OF PAGES: 24 (28 p.)

14. MONITORING AGENCY NAME & ADDRESS (if different from Controlling Office)
15. SECURITY CLASS. (of this report): Unclassified
15a. DECLASSIFICATION/DOWNGRADING SCHEDULE

16. DISTRIBUTION STATEMENT (of this Report)

Approved for public release; distribution unlimited

17. DISTRIBUTION STATEMENT (of the abstract entered in Block 20, if different from Report)

18. SUPPLEMENTARY NOTES

19. KEY WORDS (Continue on reverse side if necessary and identify by block number)

20. ABSTRACT (Continue on reverse side if necessary and identify by block number)

The radiation damage induced by the implantation of 2.7 MeV P^+ and N^+ ions with a dose of 6.4×10^{16} ions/cm^3 into GaAs at room temperature has been studied by transmission electron microscopy. The as-implanted material was found to consis of a buried amorphous layer which was sandwiched between a heavily damaged but crystalline cover layer exhibiting a high density of black dot defects, microtwins and dislocation loops and a less damaged substrate region. Post-implantation annealing of the specimens at 250°C for 6 hours resulted in the re-crystallization of the amorphous and cover layers by random nucleation of grains

DD FORM 1 JAN 73 1473 EDITION OF 1 NOV 65 IS OBSOLETE

Unclassified

SECURITY CLASSIFICATION OF THIS PAGE (When Data Entered)

401 815

producing a polycrystalline region on the single crystal substrate. However, a second stage annealing of these samples at 400°C for 2 hours caused an epitaxial regrowth of the implanted layer on the undamaged substrate producing single crystal regions which were heavily twinned on all (111) planes. The results of the present microstructural analyses have been compared with the previous infrared reflectivity studies on identically implanted GaAs samples to determine the effects of structural changes on the dielectric properties. The two studies are found to be in reasonable agreement.